Electronic Supplementary Material (ESI) for Chemical Communications.

One-dimensional and three-dimensional long-range orientation superstructures of PbSe nanocrystal

Xu Hu[a], Fulin Jia[a, b] and Jianxiao Gong*[a, b]

[a] Chinese Academy of Science (CAS) Key Laboratory of Nanosystem and Hierarchical Fabrication, CAS Center for Excellence in Nanoscience, National Center for Nanoscience and Technology, Beijing 100190, China.

[b] School of Nanoscience and Technology, University of Academy of Science, Beijing 100149, China.

*Correspondence author: gongjx@nanoctr.cn (Jianxiao Gong),

Experimental Section

Materials. lead acetate trihydrate($Pb(ac)_2 \cdot 3H_2O$, 99.999%), oleic acid(OA, 90%), 1-octadecene(ODE, 90%) and selenium(Se, 99.999%) were purchased from Sigma-Aldrich. Diphenylphospine(99%), trioctylphosphine(TOP, 99%) and octylamine (OAm, 99%) were obtained by Alfa Aesar. Toluene anhydrous (99.8%), methanol anhydrous (99.8%), ethylene glycol anhydrous and butanol anhydrous (99.8%) were purchased from Aladdin Industrial Corporation, China.

Preparation of PbSe nanocrystal. PbSe NCs were prepared using the method described by Evers et al[1]. (a) 0.595 g of lead acetate trihydrate, 30 mL of 1-octadecene and 2.2 mL of oleic acid were mixed and heated under vacuum for approximately 3 h using Schlenk line. (b) 1.12 g selenium was dissolved in a mixture of 30 mL of octadecene and 2.2 mL of oleic acid. Subsequently, solution (a) was heated to 180 ℃ under Ar and solution (b) was rapidly injected into solution (a). After 30 s, the reaction was quenched via injection of 5 mL butanol and 10 mL methanol. The crude synthesis mixtures were washed twice by precipitating with methanol, centrifugation and redispersion of the sediment in toluene. Final, the NCs were dispersed in toluene for superstructures preparation.

Preparation of PbSe superstructures. All PbSe superstructures were prepared by a modified liquid/air assembly technique in an Ar-filled glovebox (see Fig. S3). A small glass beaker was filled with 3 mL ethylene glycol, functioning as a liquid substrate. The beaker was placed in a bigger petri dish containing 4 mL of toluene. Then a volume of 300 μL of the nanocrystal suspension with initial concentration of 1.96×10^{-5} mol/L, 3.92×10^{-5} mol/L, 5.88×10^{-5} mol/L and 1.96×10^{-4} mol/L were drop-casted on top of the ethylene glycol solution, respectively, and glass beaker petri dish was covered with a bigger beaker. The evaporation of the toluene solvent and the superstructure formation was really slow and took around whole night at room

temperature. Then, the 1D linear, 2D square, 2D honeycomb, and 3D topo-epitaxy long-range superstructures of oriented attached were obtained. Meanwhile, the experimental variables for the preparation of the superstructures are listed in Table S1. Final, the dried superstructure was transferred onto substrate and TEM grid for structural characterization by dipping the sample holder vertically in/out.

For PbSe superstructures of oriented attached, the adjacent PbSe NCs are connected by the bonds between cations and anions on opposite {100} PbSe facets, which was reported in previous studies[2-4]. Since OA molecules prefer binding on {111} PbSe and {110} PbSe instead of {100} PbSe facets, when OA molecules detach from the surface of NCs, the loss of ligands occurs preferentially on {100} PbSe facets and results in anisotropic ligand distribution on NC facets. Such anisotropic ligand distribution causes alignment of NCs during self-assembly.

Table S1. The experimental variables for the preparation of the superstructures

Type	NC concentration (mol/L)	Times (h)	Temperature (℃)	Atmosphere
1D linear	1.96×10^{-5}	12	room	Ar-filled glovebox
2D square	3.92×10^{-5}	12	room	Ar-filled glovebox
2D honeycomb	5.88×10^{-5}	12	room	Ar-filled glovebox
3D topo-epitaxy	1.96×10^{-4}	12	room	Ar-filled glovebox

Characterization. TEM images and electron diffractograms were obtained using a Tecnai G2 F20 U-TWIN microscope operating at 200 kV. PbSe superstructure was scooped from the ethylene glycol interface on a carbon-coated TEM grid and dried in vacuum to remove any residual ethylene glycol. X-ray diffraction (XRD) data were collected on D/MAX-TTRIII (CBO) with Cu Kα radiation (λ = 1.542 Å) operating at 40 kV and 200 mA. Data were collected in reflection mode in the 2θ range of 10°-60° using a step size of 0.02° with scans running for 10 min. The resulting dried superstructure were transferred onto a zero-background quartz sample holder, and XRD

patterns were taken immediately after removal from the glovebox. UV-vis spectra were collected for PbSe superstructure using a Perkin Elmer Lambda 950 spectrophotometer. GISAXS measurement was performed at Xeuss SAXS/WAXS system. The AFM measurements were performed on the Bruker Multimode atomic force microscope system (Bruker, Santa Barbara, CA). The superstructures were transferred onto quartz microscope slides inside a glovebox, and Vis-NIR spectra, GISAXS and AFM were measured immediately after removal from the glovebox.

Electrical characterization. Electrical data were obtained from a PARSTANT 2273 electrochemistry workstation in nitrogen-filled glove box. Pt electrodes were evaporated on the Si wafers through a shadow mask to form a channel length (L) in 100 μm and width (W) in 500 μm. The electrical resistivity (ρ) of the superstructure was calculated by the equation:

$$\rho = \frac{RS}{L}$$

Where L is the length between two electrodes, R is the resistance obtained from I-V curve, and S is the conductor cross-sectional area.

Supporting Figures

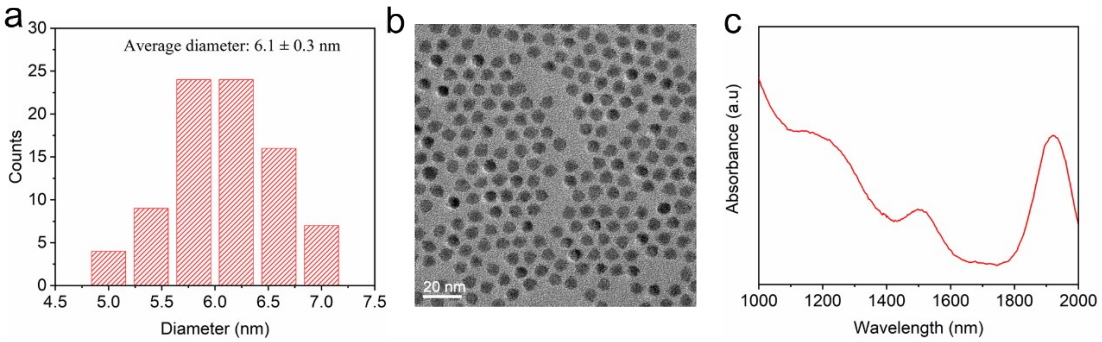

Fig. S1. (a) Statistic data of the size of PbSe NCs. (b) TEM image of PbSe NC. (c) Optical absorption spectra of PbSe NCs in dispersion. Inset: a photograph of stable colloidal solution of PbSe NCs dispersed in methylbenzene.

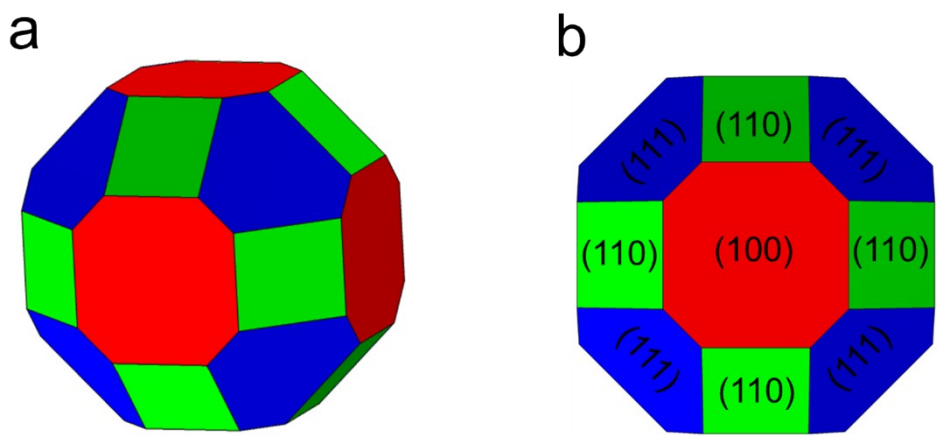

Fig. S2. (a) The truncated cube model of the PbSe NC. (b) The three types of facets: the {100} facet (red), the {110} facet (green), and the {111} facet (blue). The model has 6 {100} facets, 12 {110} facets, and 8 {111} facets. Meanwhile, the significant truncation and rhombicuboctahedron shape of PbSe NC has been shown to be fundamental for highly-ordered assemblies.

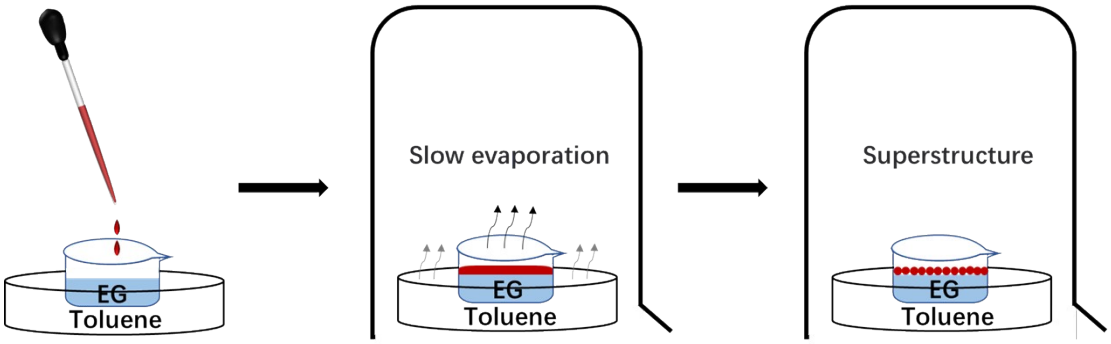

Fig. S3. Schematic representation of the superstructure preparation. This setup resulted in the gas atmosphere above the NC dispersion with a constant and large toluene partial pressure, which significantly slowed down the process of solvent evaporation and allowed the NCs enough time to find the most stable arrangement and position.

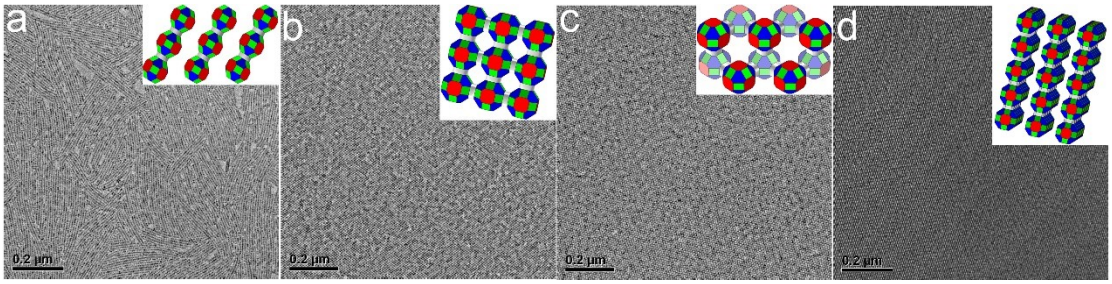

Fig. 4. Large-size TEM images of four types of PbSe superstructure: 1D line (a), 2D square (b), 2D honeycomb (c), and 3D topo-epitaxy collection (d). Inset images of (a), (b), (c) and (d) display the models of PbSe superstructure. In the model, red, blue, light green and silvery white represent the {100}PbSe facet, {111}PbSe facet, {110}PbSe facet and neck connection of PbSe NC, respectively.

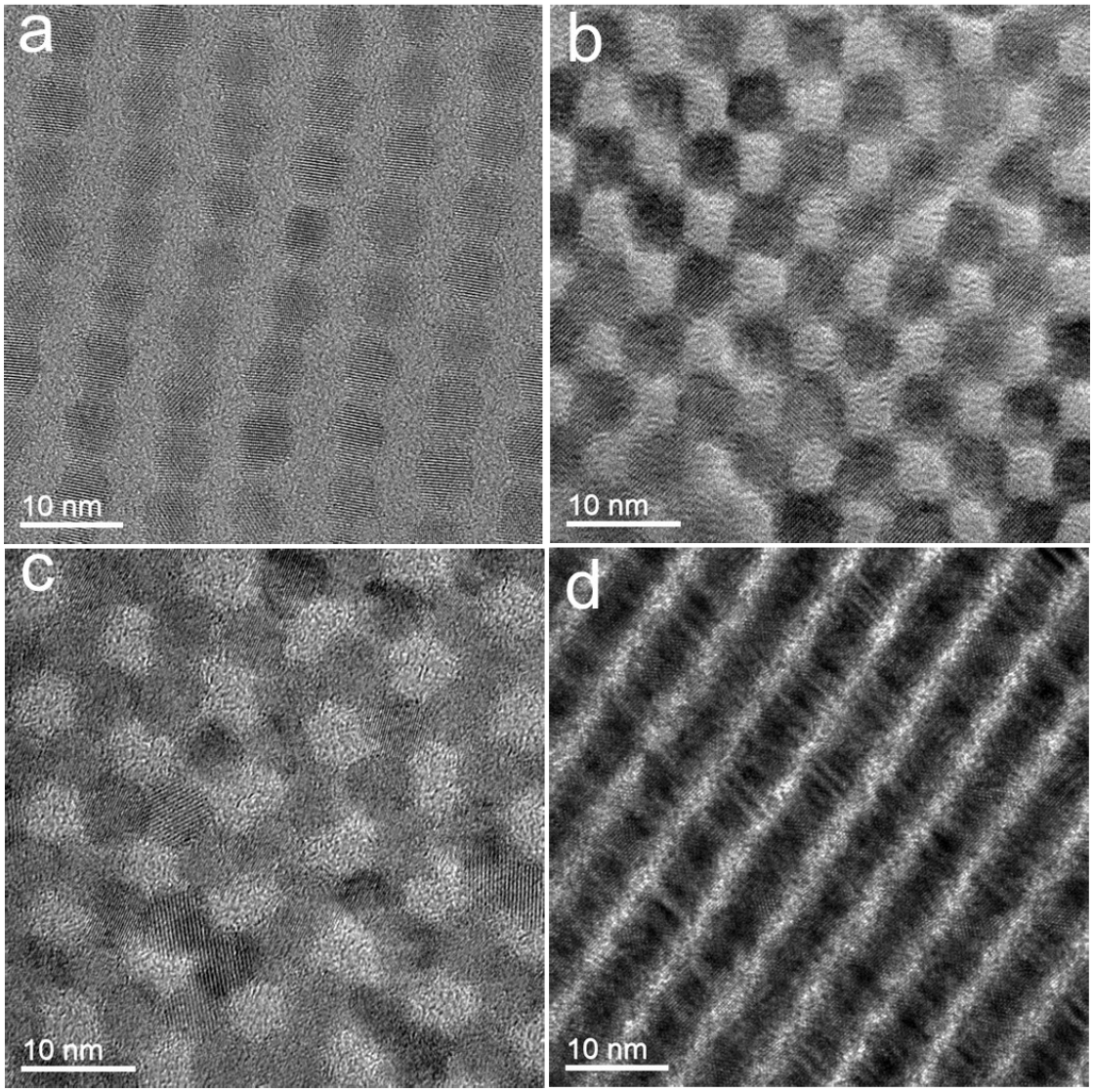

Fig. 5. High-magnification TEM images of (a) linear, (b) square, (c) honeycomb and (d) 3D topo-epitaxy superstructure of PbSe.

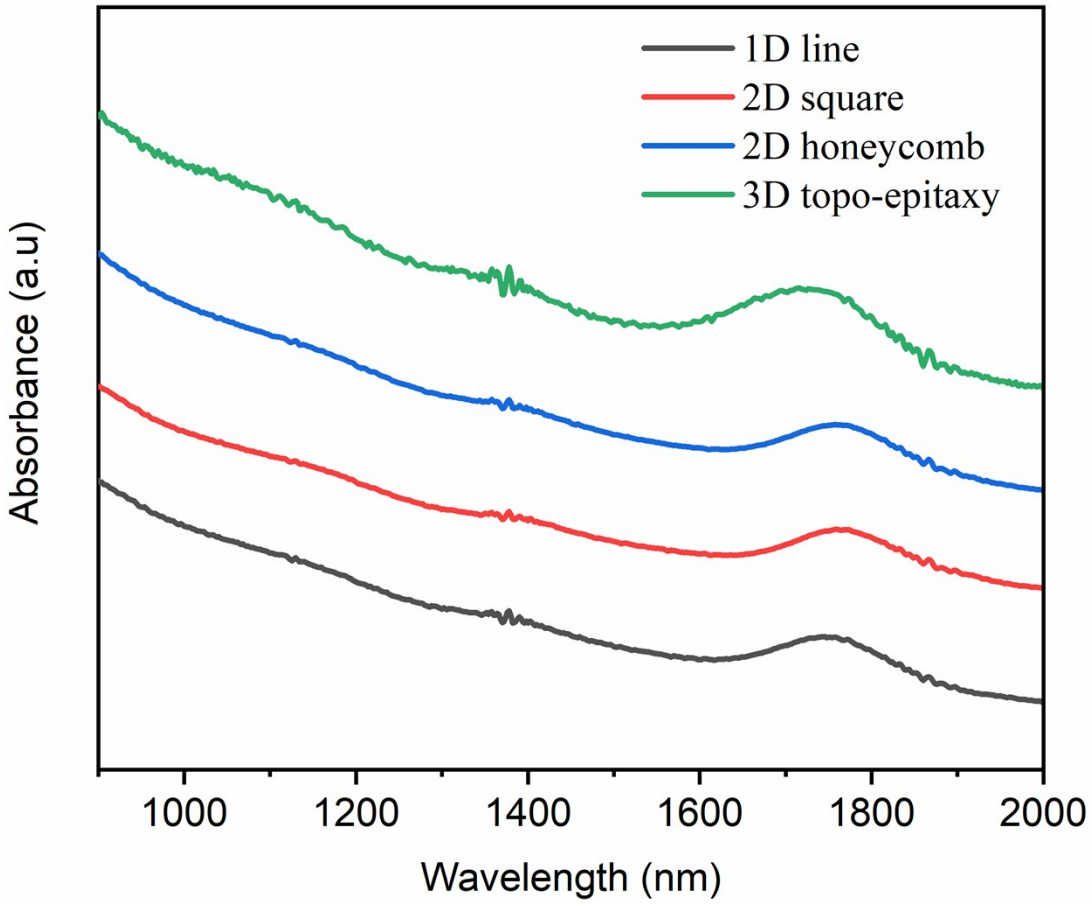

Fig. S6. UV-vis-NIR spectra of all PbSe superstructures.

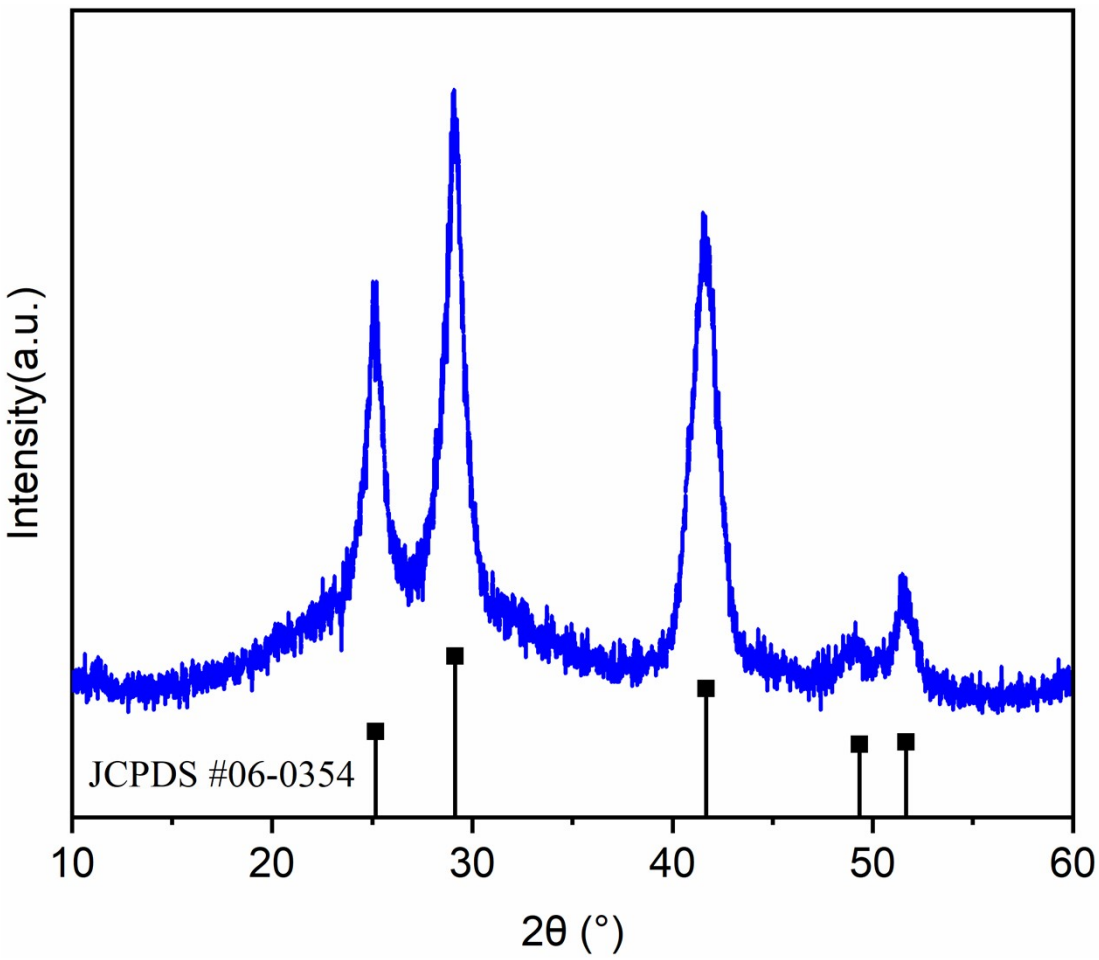

Fig. S7. Experimental XRD patterns for PbSe 3D top-epitaxy superstructures. Bottom: reference patterns for PbSe (JCPDS # 06-0354)

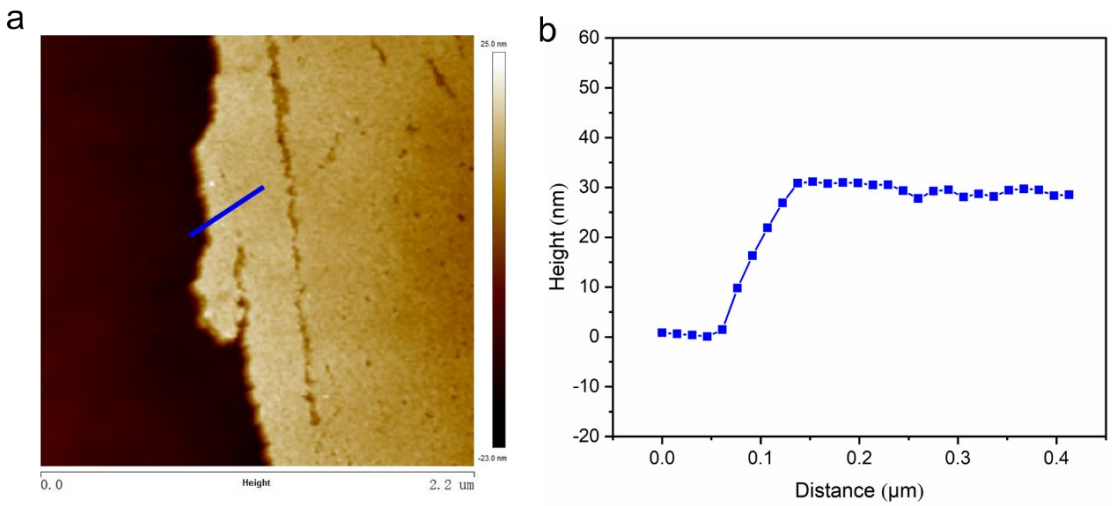

Fig. S8. (a) AFM images and (b) corresponding height profiles of PbSe 3D top-epitaxy superstructures.

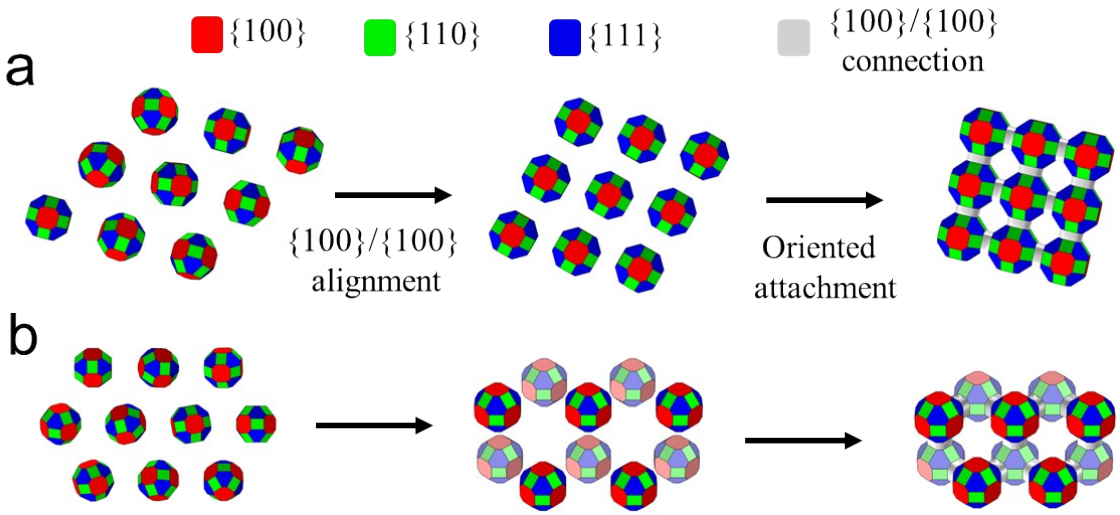

Fig. S9. Schematic illustration of self-assembly of (a) 2D square and (b) 2D honeycomb.

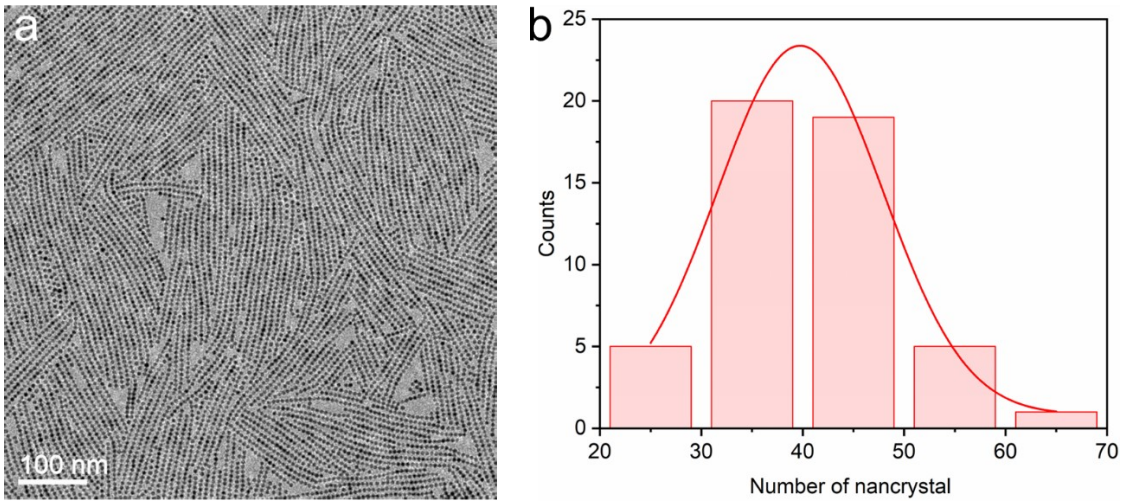

Fig. S10. (a) TEM image of 1D linear superstructure of PbSe NC. (b) Statistic data of the number of PbSe NCs in each of the 1D lines.

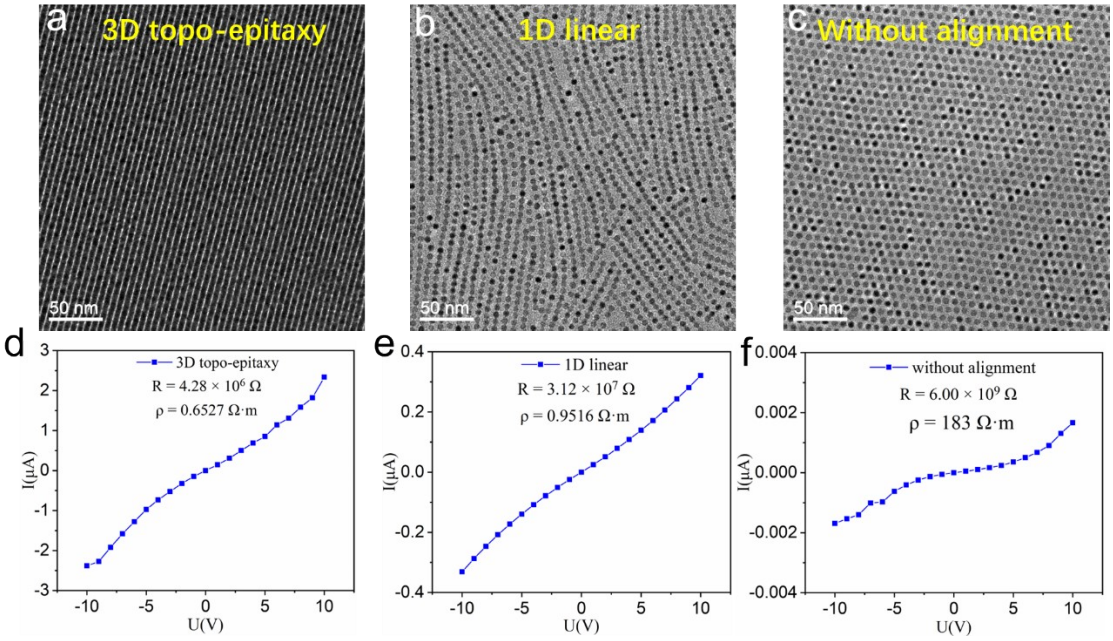

Fig. S11. TEM images and the electrical properties of 3D/1D superstructures and without alignment (a-b. TEM images; d-f. the electrical properties, therein R and ρ stand for resistance and resistivity, respectively).

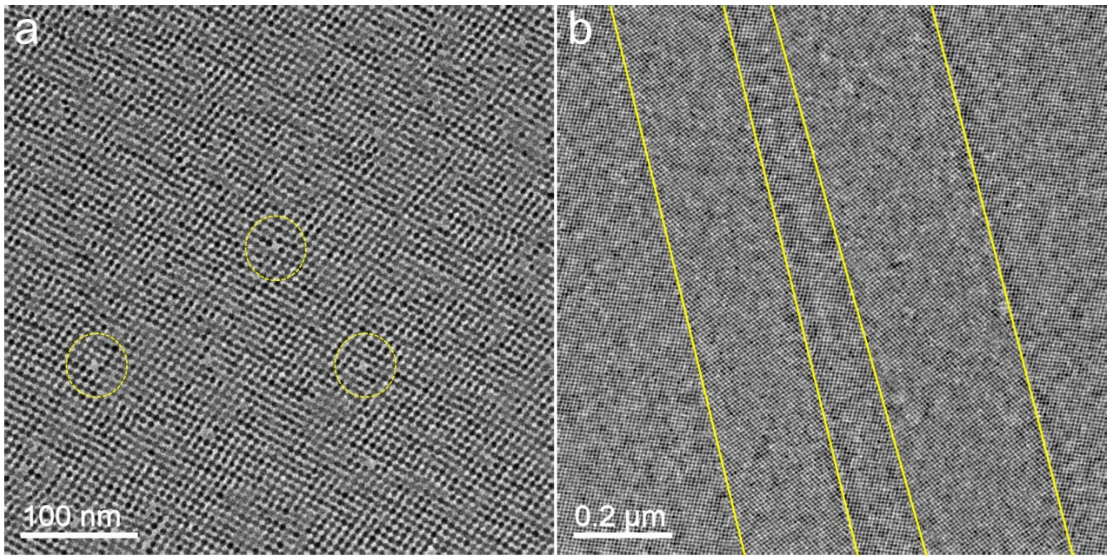

Fig. S12. Defects in the PbSe square superstructure. (a) a missing NC in the lattice. (b) grain boundary region between two lattices that had a different crystallographic orientation.

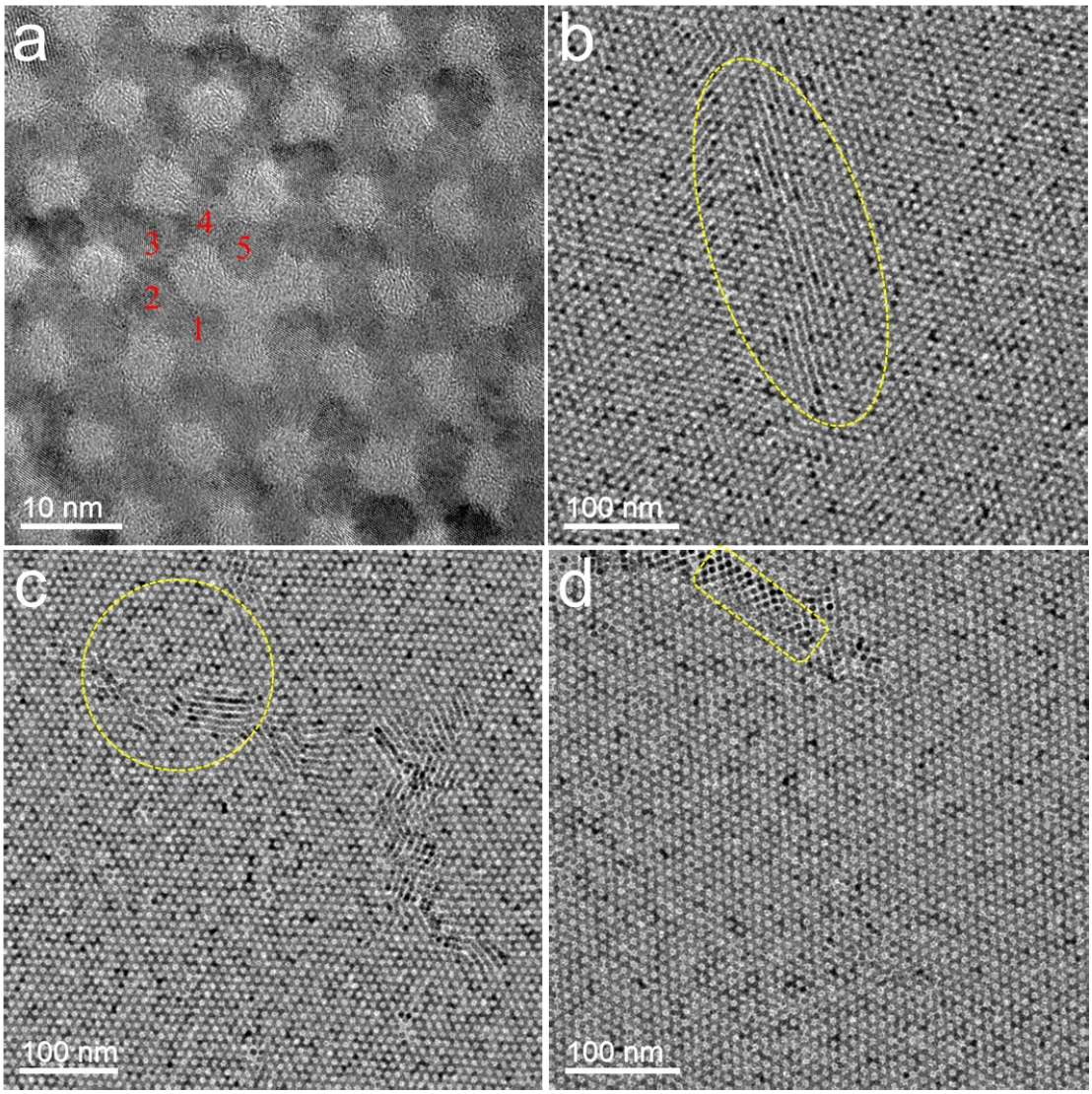

Fig. S13. Defects in the PbSe honeycomb superstructure. (a) A missing NC in the lattice. (b) and (c) One-dimensional line defect that connect nanocrystals with the same crystallographic orientation. (d) Square lattice of two nanocrystals thick.

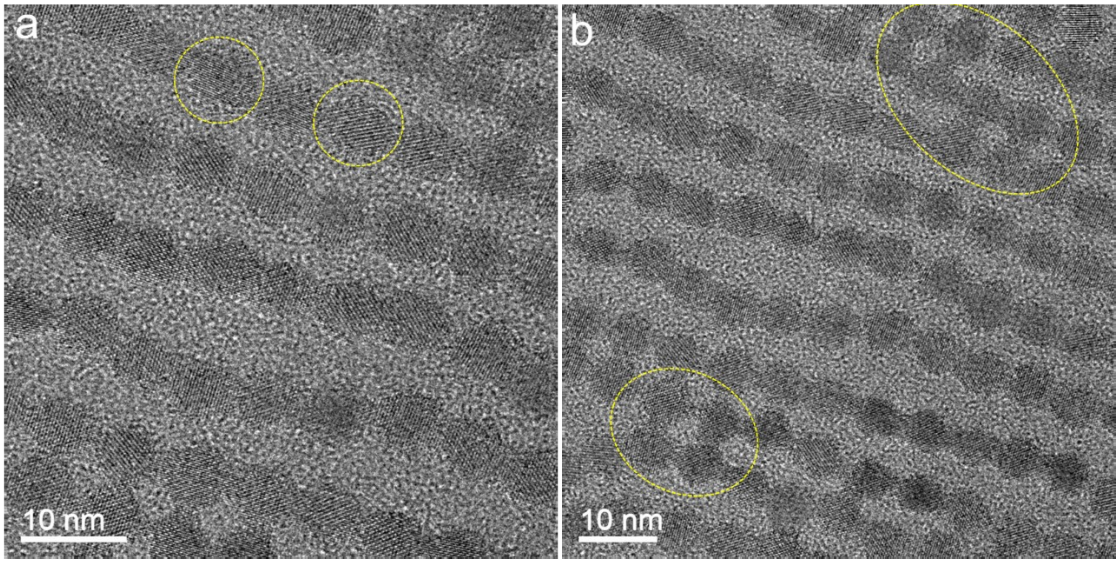

Fig. S14. Defects in the PbSe linear superstructure. (a) The single nanocrystal of {100} facet pointing up. (b) Several NCs were connected between two adjacent lines.

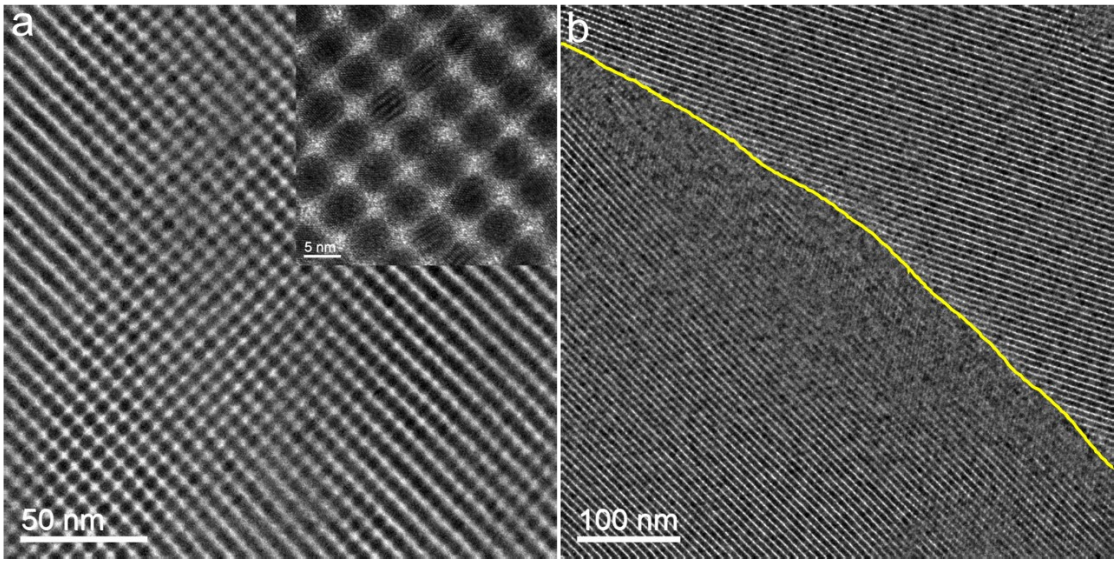

Fig. S15. Defects in the PbSe 3D topo-epitaxy superstructure. (a) Square lattice of multiple nanocrystals thick. (b) Boundaries between different domains that had a different crystallographic orientation. Inset in (a) show corresponding high-resolution TEM image.

Table S2. The relevant parameters of the structure before and after the oriented attachment

	NC-NC distance (nm)	NC-NC angle (°)	Rotational freedom
Hexagonal monolayer	L: 8.7 ± 0.4	θ: 120 ± 0.9	high
Linear superstructure	L1: 7.0 ± 0.3 L2: 9.8 ± 0.3	θ1: 103 ± 1.9 θ2: 151 ± 2.1	low

Reference:

1. W. H. Evers, B. Goris, S. Bals, M. Casavola, J. d. Graaf, R. v. Roij, M. Dijkstra and D. Vanmaekelbergh, *Nano Lett.,* 2013, **13**, 2317-2323.
2. C. M. Fang, M. A. van Huis, D. Vanmaekelbergh and H. W. Zandbergen, *ACS Nano*., 2010, 4 (1), 211-218.
3. K. Whitham, J. Yang, B. H. Savitzky, L. F. Kourkoutis, F. Wise and T. Hanrath, *Nat. Mater*., 2014, 15 (5), 557-563.
4. M. C. Weidman, Q. Nguyen, D. M. Smilgies and W. A. Tisdale, *Chem. Mater.*, 2018, **30**, 807.